

# Supercapacitor Performance of in Situ Polymerization for PANI/MnO<sub>2</sub>-TiO<sub>2</sub>

Israa Khalil Sultan ; Zaid H. Mahmoud <sup>[1]</sup>

<sup>[1]</sup> University of Diyala, College of Sciences, Chemistry Department, IRAQ

Corresponding Author: Zaid H. Mahmoud

**Abstract:-** Manganese-titanium oxide particles coated with polyaniline (PANI) have been suggested as a highly favorable electrode material for supercapacitors. The synthesis of MnO<sub>2</sub>-TiO<sub>2</sub> particles was achieved using the sol-gel technique, followed by calcination. The MnO<sub>2</sub>-TiO<sub>2</sub> was mixed with pre-synthesized PANI to create a composite material called PANI/ MnO<sub>2</sub>-TiO<sub>2</sub>. The structural composition and purity of the produced materials were verified using X-ray diffraction (XRD). The morphological analysis conducted using field emission scanning electron microscopy (FESEM) revealed that particles are securely attached to the branched-structured PANI, facilitating rapid charge transfer. The electrochemical properties of MnO<sub>2</sub>-TiO<sub>2</sub> and PANI/MnO<sub>2</sub>-TiO<sub>2</sub> were analyzed using cyclic voltammetry (CV), galvanostatic charge-discharge (GCD), 1 M H<sub>2</sub>SO<sub>4</sub> electrolyte. PANI/MnO<sub>2</sub>-TiO<sub>2</sub> demonstrated a substantial increase in specific capacity (1500 C/g) compared to PANI (450 C/g) at 1 A/g. This improvement can be attributed to the enhancement of redox-active sites and the synergistic interaction of the conductive PANI and MnO<sub>2</sub>-TiO<sub>2</sub>.

**Keywords:-** Supercapacitor, MnO<sub>2</sub>, PANI, Cyclic Voltammetry.

## I. INTRODUCTION

The study of supercapacitors, often called electric double-layer capacitors (EDLCs), is experiencing a significant surge in interest. This is mostly due to their exceptional performance as short-term power sources with high peak power capabilities. EDLCs store energy by utilizing electrostatic reactions (specifically non-Faradaic reactions) that occur between a thin layer of electrolyte separator and the surfaces of the electrode material [1-4]. The use of conductive carbonaceous materials, such as activated carbon [5], graphene [6], and carbon aerogel, is a widespread practice in this application. These materials can store energy at a significantly faster rate compared to traditional capacitors. This is because the materials have a large specific surface area, allowing them to quickly collect and release many electrolyte ions during the charging and discharging processes.

Regrettably, EDLCs are hindered by their low specific capacity, leading to a low energy density. This limitation restricts their use in applications that require consistent energy production over an extended duration. Researchers have been intensively studying the potential of hybrid supercapacitors to address this issue. These supercapacitors combine the characteristics of battery-type electrode materials with conducting carbonaceous materials to provide a synergistic effect [7-12]. In contrast to EDLCs, hybrid supercapacitors are composed of diverse electrode materials that are segregated by an electrolyte. Hybrid supercapacitors utilize EDLC-type materials for the negative electrode and battery-type materials, which store energy through Faradaic reactions, for the positive electrode. The objective is to attain a high energy density while maintaining a high power density by employing electrostatic and Faradaic processes within a single device. So far, manganese-based compounds, including manganese dioxides, manganese sulfides, and manganese carbonates, have been extensively studied as electrode materials for supercapacitors because of their strong redox characteristics. Nevertheless, using manganese phosphate as an electrode material for energy storage has yet to be extensively explored. MnO<sub>2</sub>-TiO<sub>2</sub> has demonstrated outstanding efficacy in ceramic [13-16] and anticorrosion coating applications due to its affordability, strong ion exchange capacity, and remarkable chemical and thermal stability. Regrettably, like other compounds containing transition metals, MnO<sub>2</sub>-TiO<sub>2</sub> has inadequate electrical conductivity, leading to a sluggish electron transport rate during electrochemical reactions. An effective solution to overcome the issue is combining MnO<sub>2</sub>-TiO<sub>2</sub> with a substance with comparatively greater electrical conductivity. Therefore, polyaniline (PANI), a highly conductive substance with exceptional electrical properties (subject to the specific synthesis procedures and parameters), has been chosen. By adjusting the physicochemical characteristics of MnO<sub>2</sub>-TiO<sub>2</sub> using the conductive PANI, it is possible to decrease the electrical resistance of the MnO<sub>2</sub>-TiO<sub>2</sub> material. Furthermore, PANI can provide supplementary electroactive pathways for the transport of ions, enhancing the electrochemical reversibility in redox processes [17-23].

## II. EXPERIMENTAL

A 3 ml solution of aniline and 20 ml of 1 M HCl were combined in an ice bath with vigorous stirring. Following this, 20 ml of 1 M ammonium persulphate was slowly added to the acidic solution while continuously stirring. A black-green precipitate formed and was allowed to sit in the refrigerator for 24 hours. Subsequently, the precipitate was washed until it reached a neutral pH. Finally, the precipitate was dried at 70 °C for 3h. The producer was repeat by mixing separately 3ml aniline, (20 ml, 1 M) HCl and 0.01g of MnO<sub>2</sub>-TiO<sub>2</sub>.

## III. RESULTS AND DISCUSSION

### ➤ Structural Characterization

The structural properties of PANI/TiO<sub>2</sub>-MnO<sub>2</sub> is investigated by XRD and FESEM. The XRD pattern of the as-synthesized polyaniline (PANI) is presented in **Figure 1**. The XRD analysis revealed the presence of two distinct peaks at 14.87, 20.87, and 24.98, corresponding to the (121), (113), and (322) crystallographic planes, respectively. These peaks were attributed to the periodic arrangement of PANI in directions perpendicular and parallel to the polymer chain, as reported by reference.

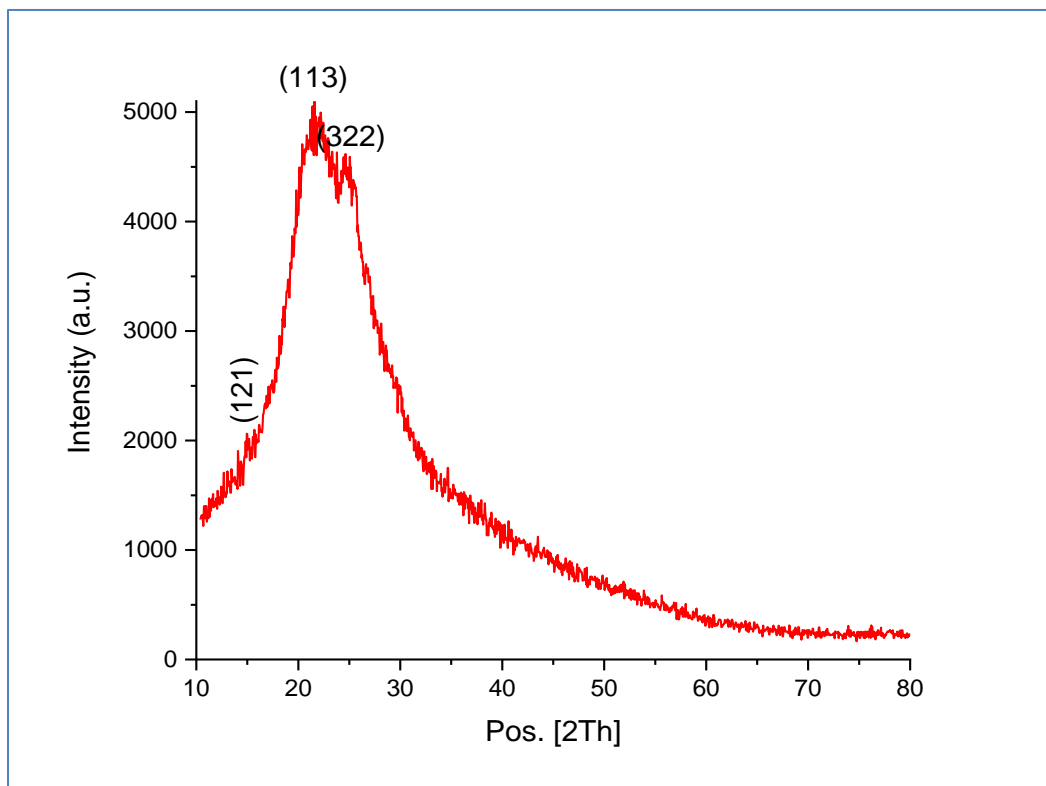


**Fig 1 XRD of Polyaniline**

The XRD pattern of the PANI/MnTiO<sub>4</sub> synthesized material is presented in **Figure 2**. Two distinct diffraction peaks corresponding to PANI were observed at 21.77 and 24.72, denoting the crystal planes (113) and (322), respectively. Similarly, two diffraction peaks at 29.42 and 36.66 were attributed to the crystal planes (310) and (211) of MnO<sub>2</sub>. Furthermore, a prominent diffraction peak at 48.34 was identified, indicating the presence of crystalline planes (200) associated with the modified TiO<sub>2</sub>.

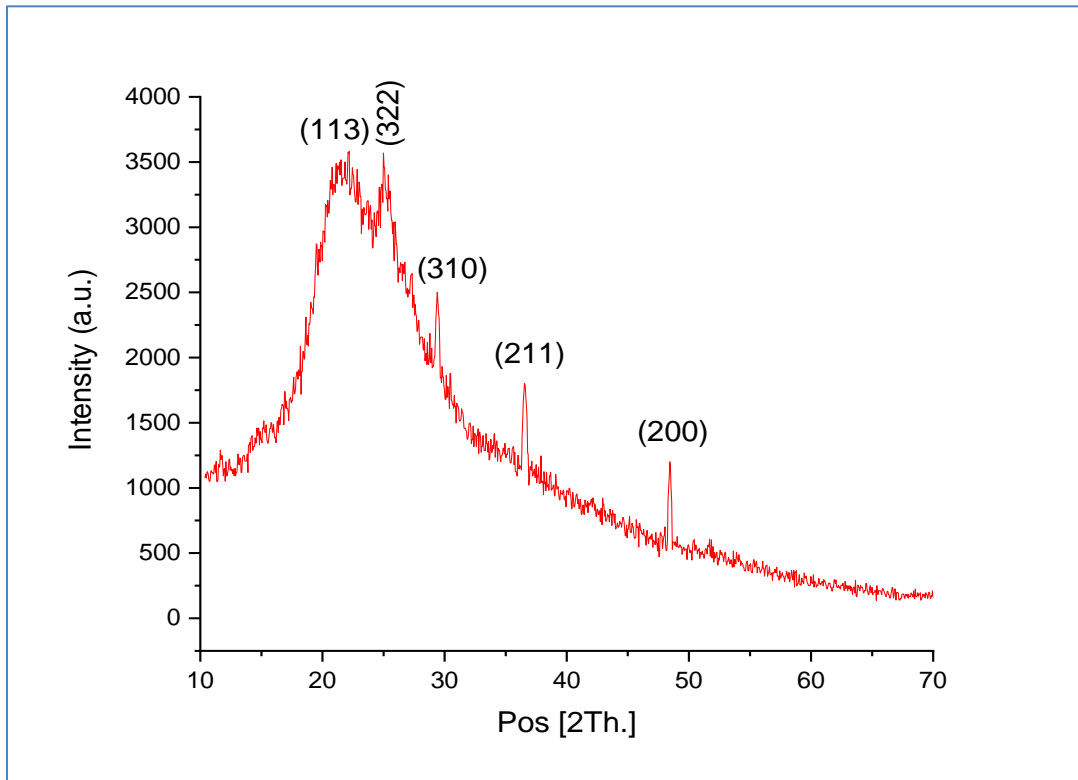


**Fig 2: XRD of PANI/TiO<sub>2</sub>-MnO<sub>2</sub>**

Figures 3 illustrate the field-emission scanning electron microscopy (FESEM) images of MnO<sub>2</sub>-TiO<sub>2</sub> integrated into a polyaniline (PANI) nanocomposite. The images demonstrate the formation of PANI/MnO<sub>2</sub>-TiO<sub>2</sub>, with the agglomeration of oxides interacting with the PANI nanotubes and covering them, indicating successful in situ-polymerization processes.

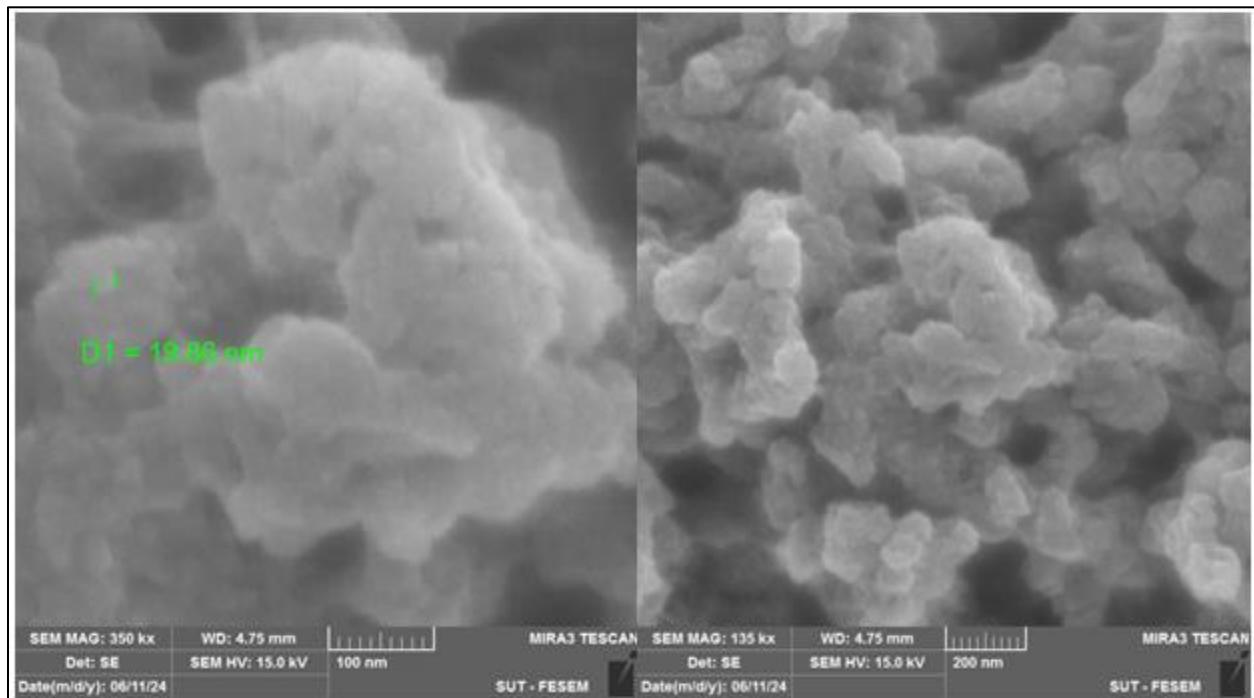


**Fig 3: FESEM of PANI and PANI/MnO<sub>2</sub>-TiO<sub>2</sub>**

➤ *Electrochemical Properties*

The study conducted galvanostatic charge–discharge (GCD) cycles on PANI, TiO<sub>2</sub>-MnO<sub>2</sub>, and PANI/TiO<sub>2</sub>-MnO<sub>2</sub> in a 1 M H<sub>2</sub>SO<sub>4</sub> electrolyte solution, varying the current (0–10 mA) and potential (0–0.9 V). The outcomes are depicted in **Figures 4**. The charge–discharge curves (CD) display inversion mirror symmetry across all current values, indicating an increase in nonlinear behavior and strong electrochemical characteristics as a pseudocapacitive with increasing current density. The discharge time decreases as the voltage drop rises due to an increase in current density, as shown in **Figure 4**. Yu et al. (2020) calculated the specific capacitance from GCD curves using Equation 1.

$$C_{sp} = \frac{I \cdot t}{V \cdot m} \quad 1$$

where m is the active material mass, I is the discharge current, Δt is the discharge duration, and ΔV is the potential window. The specific capacitance obtained from galvanostatic charge-discharge (GCD) measurements corresponds to different current densities, namely 1, 3, 7 and 10 mA, for PANI/MnO<sub>2</sub>-TiO<sub>2</sub>, TiO<sub>2</sub>-MnO<sub>2</sub>, and PANI. The specific capacitance values for these materials show significant differences across the various current densities. Notably, the addition of MnO<sub>2</sub>-TiO<sub>2</sub> binary oxide to PANI led to an improved electrode structure as evidenced by the comparison of results. The findings underscore the importance of incorporating TiO<sub>2</sub>-MnO<sub>2</sub> in creating new sites for energy storage and facilitating multiple carriers for electron transport within the electrode. The decreased internal resistance led to a notable enhancement in the electrode's efficacy for electrochemical reactions. Concurrently, it was noted that as current densities rose, the specific capacitance of the produced materials declined due to insufficient time for ions to access or reach the working electrode surface.

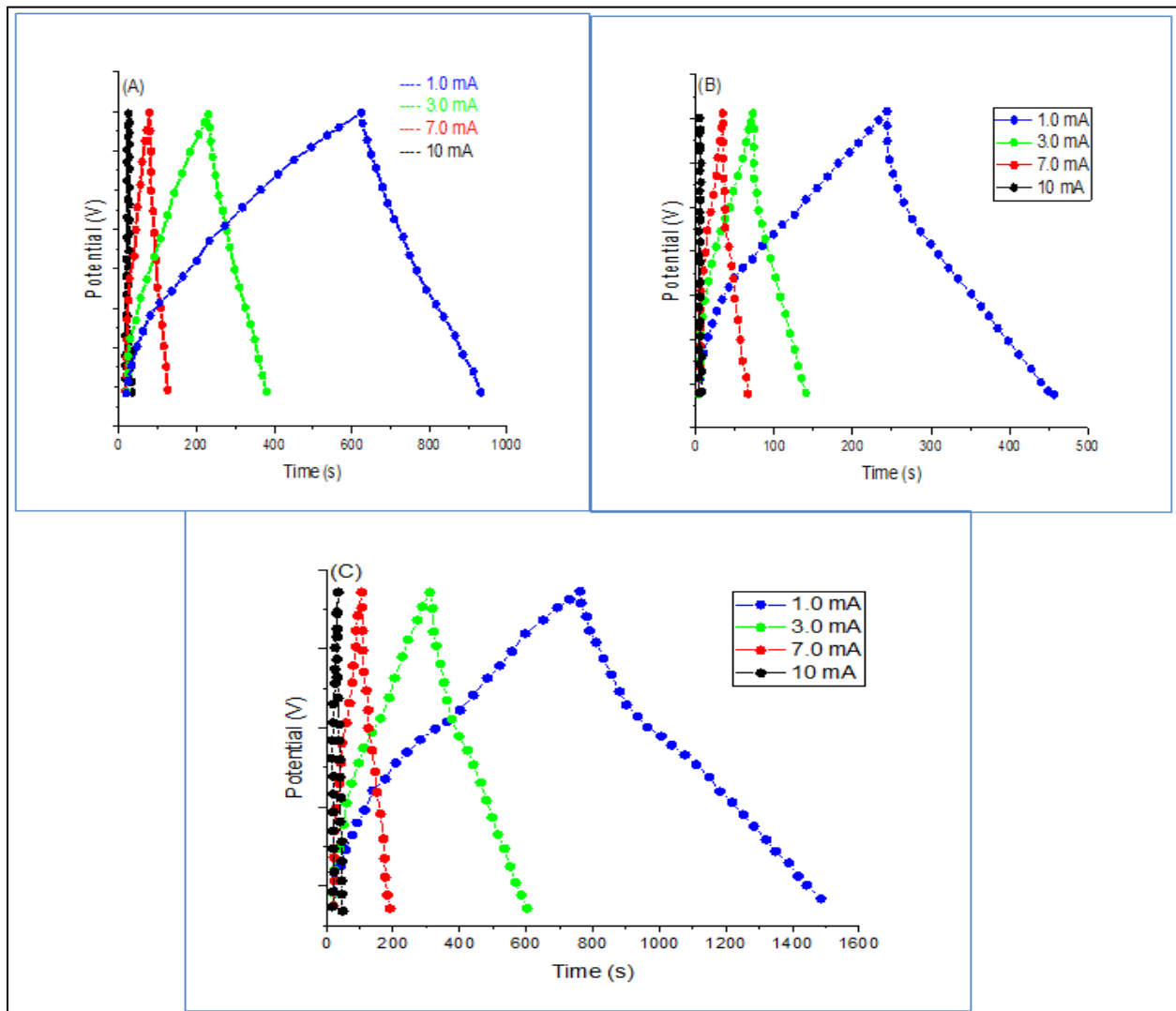


**Fig 4:** CP of PANI, TiO<sub>2</sub>-MnO<sub>2</sub>, and PANI/TiO<sub>2</sub>-MnO<sub>2</sub>

This work showed how the introduction of a binary system affected the electrical properties of PANI by conducting cyclic voltammetry (CV) measurements on PANI, TiO<sub>2</sub>-MnO<sub>2</sub>, and PANI/TiO<sub>2</sub>-MnO<sub>2</sub>. The electrochemical measurements were performed using 1 M H<sub>2</sub>SO<sub>4</sub> as the electrolyte solution. Separate experiments involved the use of three different electrode materials (PANI, TiO<sub>2</sub>-MnO<sub>2</sub>, and PANI/TiO<sub>2</sub>-MnO<sub>2</sub>) to investigate cyclic voltammetry. Cyclic voltammetry (CV) measurements were conducted at different scan rates within a potential window of 0–1.2 V, as depicted in **Figure 5**. **Figure 5a** presents the cyclic voltammetry data for PANI, TiO<sub>2</sub>-MnO<sub>2</sub>, and PANI/MnO<sub>2</sub>-TiO<sub>2</sub> at a scan rate of 10 mVs<sup>-1</sup>. The results exhibit a rectangular box shape for both electrodes, characteristic of an ideal supercapacitor with efficient charge transport. Additionally, the reduced contact resistance values indicate the pseudocapacitive nature of the electrode materials. After incorporating anatase TiO<sub>2</sub>-MnO<sub>2</sub> into the PANI/TiO<sub>2</sub>-MnO<sub>2</sub> matrix, the CV analysis of PANI/MnO<sub>2</sub>-TiO<sub>2</sub> exhibits noticeable improvement compared to PANI and TiO<sub>2</sub>-MnO<sub>2</sub>, suggesting an increase in capacitance values at the same scan rate. The CV curves in (**Figure. 5b**) depict the performance of PANI, TiO<sub>2</sub>-MnO<sub>2</sub>, and PANI/TiO<sub>2</sub>-MnO<sub>2</sub> at a scan rate of 20mVs<sup>-1</sup>. Even at high scan rates of 20 mVs<sup>-1</sup>, the redox peaks associated with the transition between leucoemeraldine, emeraldine, and emeraldine pernigraniline states of PANI demonstrate exceptional performance for PANI/MnO<sub>2</sub>-TiO<sub>2</sub>. Moreover, the findings indicate a slight shift in the anodic and cathodic peaks, which is attributed to minimal electrode resistance. The reversible reaction between the active materials of electrodes and electrolyte interfaces in the presence of 1 M of H<sub>2</sub>SO<sub>4</sub> results in changes in anodic and cathodic currents. This process, depicted in **Figure 5b**, leads to an increase in peak current separation with higher scan rates. Ghebache et al. (2021) employed a specific method to calculate the specific

capacitance of PANI, TiO<sub>2</sub>-MnO<sub>2</sub>, and PANI/MnO<sub>2</sub>-TiO<sub>2</sub> and calculated as following Equation 2.

$$C_{sp} = \frac{A}{2\gamma m(V)} \quad 2$$

where m is the active mass (g), ( $\Delta V$ ) is the potential window (V), and  $\gamma$  is the scan rate (V/s). The findings indicate that the modified PANI by TiO<sub>2</sub>-MnO<sub>2</sub> (binary oxide) exhibits higher capacitance compared to TiO<sub>2</sub>-MnO<sub>2</sub> and PANI. This is attributed to the presence of binary oxide, which enhances the structure and facilitates electrolyte accessibility by increasing surface area and enhancing polymer-binary oxide interaction. Sandip et al. (2015) observed that at different scan rates, depicted in **Figure 5C**, capacitance values decrease with increasing scan rate due to the existence of an inner active site within the electrode, preventing the capacitance from surpassing the redox transition entirely. Cycling stability is an essential property for practical applications of supercapacitors. As depicted in **Figure 5d**, GCD measurement was employed to assess the cycling stabilities of PANI, TiO<sub>2</sub>-MnO<sub>2</sub>, and PANI/TiO<sub>2</sub>-MnO<sub>2</sub> over 1000 cycles at a current density of 10A.g<sup>-1</sup>. The circular charge and discharge cycles, as well as the significant current, cause damage to the electrodes of both the pure binary system (TiO<sub>2</sub>-MnO<sub>2</sub>) and PANI. This indicates that the cycle stability of the binary system (MnO<sub>2</sub>-TiO<sub>2</sub>) and pure PANI is inferior to that of PANI/MnO<sub>2</sub>-TiO<sub>2</sub>. The MnO<sub>2</sub>-TiO<sub>2</sub> nanocomposite exhibits minimal capacitance retention after 750 cycles, with a 75% retention for pure PANI at 10A.g<sup>-1</sup>. Conversely, the PANI/TiO<sub>2</sub>-MnO<sub>2</sub> nanocomposite demonstrates robust cycling stability, retaining 91% of its initial capacitance after 1000 cycles, signifying the predominant contribution of binary oxide.

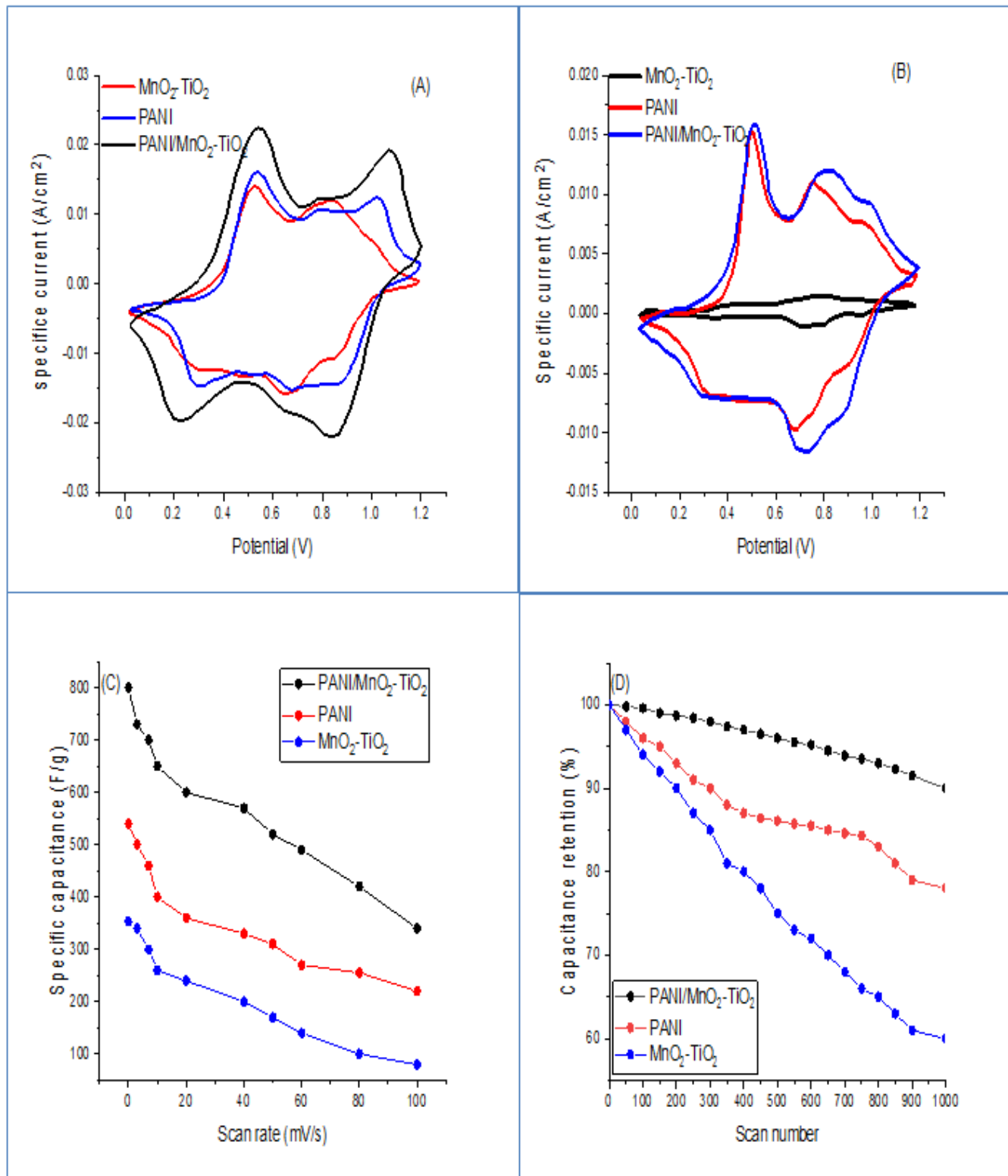


**Fig 5: CV PANI,  $\text{TiO}_2\text{-MnO}_2$ , and  $\text{PANI/MnO}_2\text{-TiO}_2$  at a Scan Rate (A) 10mV/s, (B) 20 mV/s, (C) Different Scan Rate and (D) GCD Measurement for 1000 Scan Number**

#### IV. CONCLUSION

The sol-gel approach was used to create several morphologies of the structure of MnO<sub>2</sub>-TiO<sub>2</sub>. Adding PANI to MnO<sub>2</sub>-TiO<sub>2</sub> particles improved the electrochemical performance of MnO<sub>2</sub>-TiO<sub>2</sub>. The phase structure and content were analyzed using XRD. The electrochemical performance, as evaluated using cyclic voltammetry (CV) and galvanostatic charge-discharge (GCD) experiments, shows that the specific capacity of PANI is improved compared to pure MnO<sub>2</sub>-TiO<sub>2</sub>. In addition, the battery demonstrated excellent cycling stability, with a capacity retention rate of around 80% after undergoing 1000 charge-discharge cycles at a current density of 10 A/g. Therefore, the MnO<sub>2</sub>-TiO<sub>2</sub> composite shows significant promise as a possible contender for energy storage applications.

#### REFERENCES

- [1]. Raya, I., Kzar, H.H., Mahmoud, Z.H. et al. A review of gas sensors based on carbon nanomaterial. *Carbon Lett.* 32, 339–364 (2022). <https://doi.org/10.1007/s42823-021-00276-9>
- [2]. Ashkan Bahadoran, Mahmoud Khoshnoudi Jabarabadi, Zaid Hameed Mahmood, Dmitry Bokov, Baadal Jushi Janani, Ali Fakhri, Quick and sensitive colorimetric detection of amino acid with functionalized-silver/copper nanoparticles in the presence of cross linker, and bacteria detection by using DNA-template nanoparticles as peroxidase activity, *Spectrochimica Acta Part A: Molecular and Biomolecular Spectroscopy*, 268, 2022, 120636.
- [3]. Mahmoud, Z.H., AL-Bayati, R.A. & Khadom, A.A. Synthesis and supercapacitor performance of polyaniline-titanium dioxide-samarium oxide (PANI/TiO<sub>2</sub>-Sm<sub>2</sub>O<sub>3</sub>) nanocomposite. *Chem. Pap.* 76, 1401–1412 (2022). <https://doi.org/10.1007/s11696-021-01948-6>
- [4]. Asep Suryatna, Indah Raya, Lakshmi Thangavelu, Firas Rahi Alhachami, Mustafa M Kadhim, Usama S Altimari, Zaid H Mahmoud, Yasser Fakri Mustafa, Ehsan Kianfar, A Review of High-Energy Density Lithium-Air Battery Technology: Investigating the Effect of Oxides and Nanocatalysts, *Journal of Chemistry*, 2022, 2022(1).
- [5]. Zaid H Mahmoud, Omar G Hammoudi, Ahmed N Abd, Yehya M Ahmed, Usama S Altimari, Ashour H Dawood, Riyam Shaker, Functionalize cobalt ferrite and ferric oxide by nitrogen organic compound with high supercapacitor performance, *Results in Chemistry*, 2023, 5, 100936.
- [6]. Mohammed Asaad Mahdi, Mohammed A Farhan, Zaid H Mahmoud, Ahmed Mahdi Rheima, Zainab sabri Abbas, Mustafa M Kadhim, Asala Salam Jaber, Safa K Hachim, Ahmad Hussain Ismail, Direct sunlight photodegradation of congo red in aqueous solution by TiO<sub>2</sub>/rGO binary system: Experimental and DFT study, *Arabian Journal of Chemistry*, 2023, 16(8).
- [7]. Sharaf, H.K., Salman, S., Abdulateef, M.H. et al. Role of initial stored energy on hydrogen microalloying of ZrCoAl(Nb) bulk metallic glasses. *Appl. Phys. A* 127, 28 (2021). <https://doi.org/10.1007/s00339-020-04191-0>
- [8]. M Kavitha, Zaid Hamid Mahmoud, Kakarla Hari Kishore, AM Petrov, Aleksandr Lekomtsev, Pavel Iliushin, Angelina Olegovna Zekiy, Mohammad Salmani, Application of steinberg model for vibration lifetime evaluation of Sn-Ag-Cu-based solder joints in power semiconductors, *IEEE Transactions on Components, Packaging and Manufacturing Technology*, 2021, 11(3).
- [9]. Raya, I., Widjaja, G., Mahmood, Z.H. et al. Kinetic, isotherm, and thermodynamic studies on Cr(VI) adsorption using cellulose acetate/graphene oxide composite nanofibers. *Appl. Phys. A* 128, 167 (2022). <https://doi.org/10.1007/s00339-022-05307-4>
- [10]. Mahmoud, Z.H., AL-Bayati, R.A. & Khadom, A.A. Electron transport in dye-sanitized solar cell with tin-doped titanium dioxide as photoanode materials. *J Mater Sci: Mater Electron* 33, 5009–5023 (2022). <https://doi.org/10.1007/s10854-021-07690-9>
- [11]. Zaid Hamid Mahmoud, Hanif Barazandeh, Seyed Mojtaba Mostafavi, Kirill Ershov, Andrey Goncharov, Alexey S Kuznetsov, Olga D Kravchenko, Yu Zhu. Identification of rejuvenation and relaxation regions in a Zr-based metallic glass induced by laser shock peening, *Journal of Materials Research and Technology*. 202, 11, 2015-2020
- [12]. HNK Al-Salman, Marwa sabbar Falih, Hiba B Deab, Usama S Altimari, Hussein Ghafel Shakier, Ashour H Dawood, Montather F Ramadan, Zaid H Mahmoud, Mohammed A Farhan, Hasan Köten, Ehsan Kianfar, A study in analytical chemistry of adsorption of heavy metal ions using chitosan/graphene nanocomposites, *Case Studies in Chemical and Environmental Engineering*, 2023, 8, 100426.
- [13]. Noor Sabah Al-Obaidi, Zainab Esmail Sadeq, Zaid H Mahmoud, Ahmed Najem Abd, Anfal Salam Al-Mahdawi, Farah K Ali, Synthesis of chitosan-TiO<sub>2</sub> nanocomposite for efficient Cr (VI) removal from contaminated wastewater sorption kinetics, thermodynamics and mechanism, *Journal of Oleo Science*, 2023, 72(3).

- [14]. Zaid Hameed Mahmood, Marketa Jarosova, Hamzah H Kzar, Pavel Machek, Muhaned Zaidi, Aliakbar Dehno Khalaji, Ibrahim Hammoud Khlewee, Usama S Altimari, Yasser Fakri Mustafa, Mustafa M Kadhim, Synthesis and characterization of Co<sub>3</sub>O<sub>4</sub> nanoparticles: Application as performing anode in Li-ion batteries, *Journal of the Chinese Chemical Society*, 2022, 69(4), 657-662.
- [15]. Chou-Yi Hsu, Ahmed Mahdi Rheima, Zainab sabri Abbas, Muhammad Usman Faryad, Mustafa M Kadhim, Usama S Altimari, Ashour H Dawood, Zainab Talib Abed, Rusul Saeed Radhi, Asala Salam Jaber, Safa K Hachim, Farah K Ali, Zaid H Mahmoud, Ehsan Kianfar, Nanowires properties and applications: a review study, *South African Journal of Chemical Engineering*, 2023, 46.
- [16]. Zaid Hameed Mahmood, Yassine Riadi, Hayder A Hammoodi, Ayad F Alkaim, Yasser Fakri Mustafa, Magnetic nanoparticles supported copper nanocomposite: a highly active nanocatalyst for synthesis of benzothiazoles and polyhydroquinolines, *Polycyclic Aromatic Compounds*, 2023, 43(4).
- [17]. sabri Abbas, Z., Kadhim, M.M., Mahdi Rheima, A. et al. Preparing Hybrid Nanocomposites on the Basis of Resole/Graphene/Carbon Fibers for Investigating Mechanical and Thermal Properties. *BioNanoSci.* 13, 983–1011 (2023). <https://doi.org/10.1007/s12668-023-01119-9>
- [18]. Bokov, D.O., Mustafa, Y.F., Mahmoud, Z.H. et al. Cr-SiNT, Mn-SiNT, Ti-C70 and Sc-CNT as Effective Catalysts for CO<sub>2</sub> Reduction to CH<sub>3</sub>OH. *Silicon* 14, 8493–8503 (2022). <https://doi.org/10.1007/s12633-022-01653-3>
- [19]. Saade Abdalkareem Jasim, Walid Kamal Abdelbasset, Kadda Hachem, Mustafa M Kadhim, Ghulam Yasin, Maithm A Obaid, Baydaa Abed Hussein, Holya A Lafta, Yasser Fakri Mustafa, Zaid Hameed Mahmood, Novel Gd<sub>2</sub>O<sub>3</sub>/SrFe<sub>12</sub>O<sub>19</sub>@Schiff base chitosan (Gd/SrFe@SBCs) nanocomposite as a novel magnetic sorbent for the removal of Pb(II) and Cd(II) ions from aqueous solution, *Journal of the Chinese Chemical Society*, 2022, 69(7).
- [20]. Mohammed Ahmed Mustafa, Qutaiba A Qasim, Ahmed B Mahdi, Samar Emad Izzat, Yasir S Alnassar, Emad Salaam Abood, Zaid H Mahmoud, Ahmed Mahdi Rheima, HNK Al-Salman, Supercapacitor performance of Fe<sub>3</sub>O<sub>4</sub> and Fe<sub>3</sub>O<sub>4</sub>@ SiO<sub>2</sub>-bis (aminopyridine)-Cu hybrid nanocomposite, *International Journal of Electrochemical Science*. 2022, 17(10).
- [21]. Jasim, S.A., Jabbar, A.H., Bokov, D.O. et al. The Effects of Oxide Layer on the Joining Performance of CuZr Metallic Glasses. *Trans Indian Inst Met* 76, 239–247 (2023). <https://doi.org/10.1007/s12666-022-02739-7>
- [22]. Hsu, CY., Rheima, A.M., Mohammed, M.S. et al. Application of Carbon Nanotubes and Graphene-Based Nano-adsorbents in Water Treatment. *BioNanoSci.* 13, 1418–1436 (2023). <https://doi.org/10.1007/s12668-023-01175-1>
- [23]. Hsu, CY., Al-Salman, H.N.K., Mahmoud, Z.H. et al. Improvement of the photoelectric dye sensitized solar cell performance using Fe/S–TiO<sub>2</sub> nanoparticles as photoanode electrode. *Sci Rep* 14, 4931 (2024). <https://doi.org/10.1038/s41598-024-54895-z>